Low Temperature Photochemical Vapor Deposition of SiO_2 Using 172 nm Xe_2* Excimer Lamp Radiation with Three Oxidant Chemistries: O_2, H_2O/O_2, and H_2O_2

Randa Pfeifer Roland,† Matthias Bolle,‡ and Roger W. Anderson*

Department of Chemistry and Biochemistry, University of California, Santa Cruz, California 95064

Received September 5, 2000. Revised Manuscript Received May 10, 2001

In this work, low temperature Xe_2* excimer lamp photochemical vapor deposition (photo-CVD) of SiO_2 is performed using SiH_4 with three oxidant systems: O_2, H_2O/O_2, and H_2O_2. While SiH_4/O_2 mixtures have been previously investigated, the H_2O/O_2- and H_2O_2-based chemistries are new. At 100 °C, high deposition rates can be achieved. FTIR spectra and refractive index measurements suggest that the as-deposited films have excellent stoichiometry and low hydrogen content. Our results are also used to develop a mechanistic framework for initial photodissociation reactions and subsequent chain homogeneous reactions that are important in the overall deposition chemistry. Increased gas-phase OH concentration which occurs in the H_2O/O_2 system accelerates the deposition rates, because of a chain mechanism that is operative when O_2 is available. Experimental conditions that favor reactions initiated by $O(^1D)$ instead of $O(^3P)$ have only small effects on the observed deposition rates.

Introduction

The ability to form stable, insulating SiO_2 films on Si forms the basis of planar technology for Si integrated circuits (ICs). SiO_2 is used in a wide variety of applications, including gate oxide insulators, dopant diffusion or implantation masks, device isolation structures, interlevel dielectrics, and protective layers.[1] Even as high *k* and low *k* materials are being sought for gate and intermetal (IMD) applications, respectively, the proven track record of SiO_2, particularly in terms of its chemical resistance and overall stability, will undoubtedly preserve its importance in IC applications.[2,3]

Plasma damage, contamination, and thermal budget are key concerns in industry.[2] In particular, the ability to form high-quality thin films at low temperature addresses a number of factors that contribute to device failure.[4−12] Temperatures employed for thermal SiO_2 formation exceed limits imposed by some materials, but many low temperature deposition techniques produce films of unacceptable quality. The semiconductor industry relies heavily on reduced-temperature plasma-enhanced deposition methods and thermally driven organosilicon-based chemical vapor deposition (CVD) techniques; however, each method suffers from drawbacks. Sputtering, also a widely used low temperature technique to deposit SiO_2, involves ablating precursors from a solid target in a low pressure environment, sometimes in the presence of reactive gases. As sputtering relies on quite different methodologies and involves a different set of problems, it will not be discussed. Nonplasma, low temperature deposition methods are also of great interest in many other advanced technologies, including ULSI circuits, solar energy cells, flat panel displays, and optical systems.[10,13] Photochemical vapor deposition (photo-CVD) represents a low temperature alternative that has yet to find widespread application. Since the late 1970s, high-quality elemental and compound films have been formed by photo-CVD, with the added benefits of spatial resolution, chemical specificity, and reduced temperature.[14] More independent control of process parameters generally translates into easier optimization and a broader process window than conventional deposition methods.[15]

SiO_2 is the most widely applied and characterized photo-CVD dielectric,[14] with films often showing good step coverage, low interface state and defect densities, and low stress levels. The overall film quality is comparable or superior to that obtained by thermal and plasma-enhanced methods.[14,15] Previous photo-CVD work has relied primarily upon low pressure mercury lamps and ArF excimer lasers, with vacuum ultraviolet

* Corresponding author. E-mail: anderson@chemistry.ucsc.edu.
† E-mail: pfeifer@ chemistry.ucsc.edu.
‡ E-mail: drmabo@gmx.de.

(1) Franke, J. E.; et al. *Spectrochim. Acta* **1994**, *50A*, 1687.
(2) SEMATECH. *The International Roadmap for Semiconductors*, 1999 ed.; Semiconductor Industry Association: San Jose, CA, 1999; http://www.itrs.net/1999_SIA_Roadmap/Home.html. See also: SEMATECH. *The National Technology Roadmap for Semiconductors*, 1997 ed.; Semiconductor Industry Association: San Jose, CA, 1997; http://notes.sematech.org/ntrs/PublNTRS.nsf.
(3) Baliga, J. *Semicond. Int.* **1998**, June, 139.
(4) Haque, M. S.; et al. *J. Electrochem. Soc.* **1997**, *144*, 3265.
(5) Strass, A.; et al. *Thin Solid Films* **1999**, *349*, 135.
(6) Eden, J. G. *Photochemical Vapor Deposition*; Wiley-Interscience: New York, 1992.
(7) González, P.; et al. *Thin Solid Films* **1992**, *218*, 170.
(8) Kazor, A.; Boyd, I. W. *Appl. Surf. Sci.* **1992**, *54*, 460.
(9) Ray, S. K.; et al. *J. Mater. Sci.* **1990**, *25*, 2344.
(10) Cote, D. R.; et al. *IBM J. Res. Dev.* **1999**, *43*, 5.
(11) Homma, T. *Mater. Sci. Eng.* **1998**, *23*, 243.
(12) Nguyen, S. V. *IBM J. Res. Dev.* **1999**, *43*, 109.
(13) Boyd, I. W. *Mater. Sci. Forum* **1995**, *173−174*, 81.
(14) Eden, J. G. *Photochemical Vapor Deposition*; Wiley-Interscience: New York, 1992.
(15) González, P.; et al. *Thin Solid Films* **1992**, *218*, 170.

10.1021/cm0007095 CCC: $20.00
Published on Web 07/06/2001

(VUV) emission at 185 and 193 nm, respectively. Each light source has disadvantages. Mercury lamps are generally low intensity, which can translate into low deposition rate(s), r_d(s). Excimer lasers provide high power density, but a provision must be made to move the laser beam or the substrate for deposition over large areas. Films deposited from a variety of precursors at very low temperatures (less than 200 °C) sometimes show low r_d's, low refractive indices, inferior optical quality, and poor adherence, but results suggest that further research is warranted.[14,15]

Xe_2* excimer lamps provide intense radiation at 172 nm and represent a promising light source for photo-CVD applications. With regard to SiO_2 deposition, Bergonzo and Boyd, et al., have reported high r_d's using O_2 and SiH_4 at lamp intensities of 20 mW/cm^2. At 200 °C, r_d's ranged between approximately 65 and 200 Å/min with SiH_4:O_2 ratios under about 7:100;[16,17] at 300 °C, r_d's were roughly 100−400 Å/min. Films deposited at the higher r_d's tended to be very porous (e.g., Si−O−Si FTIR absorption at 1065 cm^{-1} with 110 cm^{-1} fwhm, low refractive index, high etch rate, possible Si−H contamination).[16] A large degree of hydrogen (>5%) was incorporated into the films when temperatures between 100 and 200 °C were employed.[16] The film properties obtained at high r_d's suggest that gas-phase reactions are producing $Si_xO_yH_z$ species that are too large to react effectively at the surface to produce the desired SiO_2 material. This could be due to either long residence times or relatively high light intensity; however, based on the information given, it is difficult to ascertain which might be dominant.

N_2O has also been used with SiH_4, but r_d's were significantly lower (often 15 Å/min or less at 250−300 °C), in part because the absorption cross section of N_2O at 172 nm is over an order of magnitude smaller than O_2, and N_2O photolysis produces only one O atom (albeit O(^{1}D)). Powder formation has also been problematic, even at SiH_4:N_2O ratios as low as 2:100,[18,19] and films often shown high porosity, low density, N contamination, and/or O deficiency.[19]

It is difficult to compare our research with that reported by other investigators for a number of reasons. First, the reports are silent regarding the residence time of the reactants in the deposition chambers. Specification of residence times must be part of the photo-CVD work because long residence times favor thermal reactions that contribute to gas-phase nucleation of both thermally and photochemically generated species. Second, it is not clear how well the reactants are confined above the wafer surface. Hence, there may be a large spread in residence times because the reactants may swirl and eddy a great deal before they are evacuated. Both of these factors can lower film quality. Third, light intensity at the wafer surface is not always given. Fourth, the information provided regarding specific reaction conditions is not sufficient. Fifth, consideration must be taken for the differences in temperature. Photo-CVD experiments performed at temperatures at or above 200°C generally produce both photochemical and thermal processes unless the residence time is sufficiently short.

Primary goals of our work include the following: developing practical, low temperature processes to synthesize high-quality silicon oxide based dielectric materials; gaining more understanding of the chemical reaction mechanism; characterizing the thin film materials; using our mechanistic models to develop new photo-CVD processes for other materials. FTIR and refractive index data indicate that good-quality SiO_2 is deposited at reasonable r_d's and very low temperatures without high temperature annealing. As deposited, the films show Si−O−Si stretching absorption peaks in excess of 1070 cm^{-1} and refractive indices around 1.45. These values are comparable to those of high-quality thermal oxides. Using the 172 nm provided by a Xe_2* excimer lamp opens up the possibility of exploring alternative oxidants that do not absorb well at slightly longer VUV wavelengths. In our work, we find contributions to the deposition from thermally induced reactions only for temperatures greater than 150 °C. Hence, substrate temperature is maintained at 100 °C or below to ensure that film formation is photochemically driven (i.e., thermal deposition was negligible). System parameters related to gas flow and residence times that are ignored or not specified by many other research laboratories receive close attention.

Experimental Section

The deposition apparatus is similar to many CVD chambers but is modified to allow irradiation of the substrate by the light source. The VUV lamp (Heraeus Nobelight Xe_2* excimer lamp) is located about 20 cm above the substrate, and we estimate from our actinometry results that the intensity at the wafer surface is about 2 mW/cm^2.[20] Reactant gases flow over the substrate from the upstream side, and the lamp is purged by a downward gas flow to prevent deposition on the lamp surface. Gas flows are managed by means of several vanes that confine the reactant gas flows to a region about 1.2 cm above the substrate. The vanes also limit the irradiated region of the substrate to about 50 mm. Unreacted gases and volatile reaction products are pumped away with a Roots blower/mechanical pump combination. Because SiH_4 has the potential to ignite spontaneously in air, any unreacted SiH_4 is removed from the exhaust by means of a scrubber using aqueous NaOH.

Cylinders provide the permanent reactant gases (Ar, O_2, and 15% SiH_4 in N_2 or Ar), and they are used without further purification. Boiloff from liquid N_2 provides the N_2 gas. Because of the hazards associated with SiH_4 compressed gas, all normal safety considerations, such as storing the cylinder in a ventilated, sprinklered gas cabinet, are employed. Gases are delivered to the deposition chamber with 12 computer controlled mass flow controllers. Liquid reactants (H_2O and 30 wt % H_2O_2) are delivered with a Beckman HPLC pump at liquid flow rates from 0.1 to 0.3 mL/min. Chamber pressure is measured with capacitance manometers and is controlled by the computer with a MKS butterfly valve. The overall gas flows of O_2, H_2O_2, and H_2O are given in the second column of Table 1, and the SiH_4 flow is either 22.5 sccm (standard cubic centimeters per minute) or 11.25 sccm. The reactant gases are diluted in about 3400 sccm N_2 or Ar. The reactant gases are confined to a channel that is 28 cm wide and 1.2 cm high. Under these conditions, the potential hazard of developing explosive SiH_4−oxidant mixtures is negligible.

SiO_2 is deposited onto 100 mm Si wafers positioned below the lamp on a stage that could be heated to 400 °C by means

(16) Bergonzo, P.; Boyd, I. W. *J. Appl. Phys.* **1994**, *76*, 4372.
(17) Bergonzo, P.; Boyd, I. W. *Electron. Lett.* **1994**, *30*, 606.
(18) Bergonzo, P.; et al. *Appl. Surf. Sci.* **1993**, *69*, 393.
(19) González, P.; et al. *Thin Solid Films* **1993**, *421*, 348.
(20) Roland, R. P.; Bolle, M.; Anderson, R. W. *J. Phys. D* **1998**, *31*, 1336.

Table 1. Average Deposition Rates for the O_2, H_2O/O_2, and H_2O_2 Deposition Systems

		deposition rate (Å/min)			
oxidant	flow (sccm)	7 Torr	5 Torr (slow)[a]	5 Torr (fast)	1/2 SiH_4
O_2	200	35			
	300	53	26	28	35
	400	134	37	42	
H_2O/O_2	120/100	110			
	120/200	137			
	120/300	143			
H_2O/O_2	240/50[b]	9			
	240/100	143			
	240/200	187	109	143	125
	240/300	211	119	160	
H_2O/O_2	360/100	169			
	360/200	239	140	171	
	360/300	259	150	194	
H_2O_2	120	75			
	240	156	111	134	120
	360	225	174	181	194

[a] The flow rates indicated are actually lower by a factor of 5/7, or 0.71. [b] Nonlinearities in the mass flow controller become evident at such a low flow rate.

of quartz IR lamps. Standard operating temperature and pressure are 100 °C and 7 Torr. Two types of experiments are conducted at 5 Torr: one ("slow") with most gas flow rates scaled by the ratio of the pressures (i.e., 5/7 = 0.7); one ("fast") with the flows used at 7 Torr. In most cases, N_2 serves as the purge gas. Unless specified, SiH_4 flow rate is 22.5 sccm (150 sccm flow of 15% SiH_4 in inert gas). Liquid precursor flow rates are presented as the sccm gas flow rate equivalent to the set liquid flow in ml/min.

Fifty millimeters of the substrate is directly irradiated; any light reflected into the downstream half of the active deposition region probably extended no more than 10 mm. Experiments performed with spin-on precursors also suggested that reflections might contribute up to about a third of the light intensity at the level of the wafer. Reactant and purge gases are added in a "sequential" manner, such that nominal gas flow velocities across the wafer did not change. Accounting for the additional gases added in the irradiated region, a reasonable plug flow velocity for the reacting gases is 300 cm/s. This translates into residence times prior to, during, and downstream of the exposure to VUV radiation of approximately 10, 21, and 17 ms, respectively. The process gases, which are vertically confined to roughly 1.2 cm above the deposition surface, are "optically thin" (i.e., a small percent of the light is absorbed). On the basis of known rate constants and calculated effective reactant concentrations, it appears that SiH_4 is mostly depleted by the time that gases pass over the wafer. H_2O_2 and O_2 concentrations might fall by as much as 25% due to combined reactions, and the H_2O concentration seems to increase. The concentrations of the other reactants appear to remain relatively unchanged.

Thickness data are generated from ellipsometric analysis ($\lambda = 635$ nm; $\eta = 1.45$) using a locally built ellipsometer, and average r_d's in angstroms per minute are calculated using thickness data points measured over a 51 mm × 18 mm region on the wafer exposed to the VUV radiation. Because we have found that r_d appears to increase linearly with lamp output under our conditions, all r_d's are scaled to correct for small differences in average light intensity experiment to experiment. The linear relationship was determined by comparing the scaled results of standard runs repeated periodically during the course of our experiments and confirming their correspondence. When desired, reaction conditions can be optimized such that the thickness variation over the entire Si wafer is around 1−2%.

FTIR spectra of films are obtained using a Mattson Galaxy 4020 FTIR spectrometer coupled with First v. 1.0 software at a resolution of 2 cm^{-1} and taking 128 scans per spectrum. Minimum film thickness of about 4500 Å is required to obtain usable spectral data. Background noise due to water in some spectra is intrinsic to the spectrometer, not to water trapped in or absorbed by the films. Difficulties with analysis also arise due to variations in wafer quality and doping levels, combined with spectrometer-related noise. The reliability of the spectra above about 3200 cm^{-1} is poor, and subtraction of the blank wafer tends to distort the broad absorption peak in the 3200−3600 cm^{-1} region, making the OH concentration appear to artificially increase. Despite these factors, spectra are qualitatively compared, and H and OH levels are estimated.

Mechanism of SiO_2 CVD

The reaction mechanism underlying SiO_2 CVD (both thermal and photochemical) has been the subject of a great deal of speculation but not much quantitative work. When SiH_4 and an oxidant such as O_2 are used for thermally driven processes, it has been suggested that film growth is the result of heterogeneous reactions that occur on the deposition surface.[21,22] A different deposition mechanism hinges on the hypothesis that deposition originates with an intermediate formed by homogeneous reactions between SiH_4 and O_2. The latter case is more likely, such that SiH_4 oxidation proceeds through a chain process where the reaction SiH_3 with O_2 molecules plays a key role because it can produce a variety of partially oxidized SiO_xH_y intermediates, such as HSiOOH, SiH_2O, and/or SiH_3O, as well as active chain carriers, such as H, OH, and O.[23−25] The critical temperature (i.e., the temperature at which deposition begins) and r_d's tend to show a marked dependence on parameters such as temperature, O_2:SiH_4 ratios, SiH_4 flow, total gas flow rate, and pressure, as well as reactor design, gas flow patterns, and so on.[23,26,27] Lower temperatures typically result in unacceptable film quality as well as negligible deposition rates.[15]

Although photochemically activating reactants using VUV radiation represent a promising low temperature way to deposit good-quality SiO_2 at reasonable r_d's, no general theory for SiO_2 photo-CVD is available. There is some disparity in the data reported by different groups. Deeper kinetic studies, in situ analysis, control of interface phenomena, and study of the early stages of deposition have been recommended.[15] However, as we show in our modeling paper, known chemical reactions provide a good understanding of our experiments.[28]

Although 172 nm light provides more than twice the average energy of a Si−H single bond (696 and 293 kJ/mol, respectively),[29,30] SiH_4 is transparent to light of wavelengths longer than roughly 150 nm.[31,32] SiH_4 is susceptible to H atom abstraction by a variety of oxidants, such as O and OH. Once SiH_3 is formed, its reaction with O_2 could then enhance oxidation reactions via the branching-chain mechanism.[23] Common com-

(21) Baliga, B. J.; Ghandhi, S. K. *J. Appl. Phys.* **1973**, *44*, 990.
(22) Bennett, B. R.; et al. *Appl. Phys. Lett.* **1987**, *50*, 197.
(23) Ojeda, F.; et al. *J. Mater. Res.* **1998**, *13*, 2310.
(24) Vasiliev, V. V.; et al. *Thin Solid Films* **1981**, *76*, 61.
(25) Vasiliev, L. L.; et al. *Thin Solid Films* **1978**, *55*, 221.
(26) Goldsmith, N.; Kern, W. *RCA Rev.* **1967**, *28*, 153.
(27) Strater, K. *RCA Rev.* **1968**, *29*, 618.
(28) Roland, R. P.; Anderson, R. W. *Chem. Mater.* **2001**, *13*, 2501.
(29) Jasinski, J. M.; et al. *Chem. Rev.* **1995**, *95*, 1203.
(30) Cotton, F. A.; Wilkinson, G. *Advanced Inorganic Chemistry*, 2nd ed., Wiley-Interscience: New York: 1966; Vol. 100, pp 456−485.
(31) Robin, M. B. *Higher Excited States of Polyatomic Molecules*; Academic Press: New York: 1975; Vol. 2, p 298.
(32) Harada, Y.; et al. *Chem. Phys. Lett.* **1968**, *1*, 595.

pounds, such as O_2, O_3, H_2O, and H_2O_2, have relatively high absorption coefficients in the VUV[33] and undergo photodissociation at low temperatures to produce OH and O, initiating a reaction sequence that leads to SiO_2 formation. While SiH_4 and O_2 have been used by other researchers as precursors for SiO_2 photo-CVD, this represents the first study using the reaction mixtures $SiH_4/H_2O/O_2$ and SiH_4/H_2O_2.

O_2 photodissociates into oxygen atoms with an absorption cros section σ_{172} of roughly 20 atm^{-1} cm^{-1} at 172 nm.[33,34] Radiation of wavelength less than 240 nm generates two $O(^3P)$; for wavelengths less than 175 nm, $O(^1D)$ is produced:

$$O_2 + h\nu(\lambda \leq 249\ \text{nm}) \rightarrow O(^3P) + O(^3P)$$

$$O_2 + h\nu(\lambda \leq 175\ \text{nm}) \rightarrow O(^1D) + O(^3P)$$

The precise branching ratio at 172 nm is not clear, but based on the potential energy curves of low-lying electronic states in O_2 (i.e., $X^1\Sigma_g^-$, $a^1\Delta_g$, and $b^1\Sigma_g^+$),[35] $O(^1D)$ production is an allowed process and may account for as many as 50% of the atoms produced by photodissociation.[36] Secondary reactions in O_2 photochemistry generate O_3 by means of a reaction of O, O_2, and a third body.[35] However, under our conditions, based on the well-known Chapman mechanism, the rate of O_3 production via a three-body process is slow and never effectively competes with the fast, bimolecular reaction of SiH_4 and O. Consequently, more than 99.9% of the O atoms produced should react with SiH_4, so we ignore any possible involvement of O_3 photochemistry.

H_2O possesses a σ_{172} of roughly 100 atm^{-1} cm^{-1}, 5 times greater than that of O_2 and O_3.[35,37] The primary photoprocess in the 140−190 nm region generates H and OH radicals, thereby providing a direct link to a highly aggressive oxidant.[35] OH is thought to be the strongest oxidant of the oxygen radical family (OH, OR, O, HOO, ROO, RC(O)O).[38] Aside from H_2O, H_2O_2 is the only other stable molecule containing only hydrogen and oxygen. Vaporization of 30 wt % aqueous solution of H_2O_2 provides a third type of photochemical oxidant. Its UV photolysis forms two OH radicals ($\sigma_{172} = \sim 80$ atm^{-1} cm^{-1}),[39] initiating a series of reactions that culminate in the production of H_2O and O_2.[40−43]

The initial reactions in the gas-phase chemistry play a large role in shaping the overall mechanism leading to film deposition. Reactions that may be proposed include

$$SiH_4 + O(^3P) \rightarrow SiH_3 + OH \quad (1)$$

$$SiH_4 + OH \rightarrow SiH_3 + H_2O \quad (2)$$

$$SiH_3 + O_2 \rightarrow SiH_3O_2^* \quad (3)$$

These reactions are undoubtedly fast, but there is some discrepancy in the literature in terms of the rate constant for reaction 1. Room-temperature values range between about 3.2×10^{-13} and 1.2×10^{-12} cm^3 $molecule^{-1}$ s^{-1}.[44,45] Reactions 2 and 3 are at least an order of magnitude faster than reaction 1, with k_2 and k_3 equal to approximately 1.4×10^{-11} and 1.3×10^{-11} cm^3 $molecule^{-1}$ s^{-1}, respectively.[44−47] In terms of deposition chemistry, H_2O and H_2O_2 photolysis make more OH available more quickly than the O_2 system; the OH radicals can rapidly abstract H from SiH_4 to form SiH_3, which is subsequently susceptible to fast attack by O_2. The $SiH_3O_2^*$ formed can decompose via a number of channel pathways:[16,29,47−51]

$$SiH_3O_2^* \rightarrow SiH_2O_2 + H \quad (4a)$$

$$\rightarrow SiH_2O + OH \quad (4b)$$

$$\rightarrow H_3SiO + O \quad (4c)$$

Although Koshi et al. have measured the branching ratio for reactions 4a, 4b, and 4c to be 0.65, 0.25, and 0.10, respectively,[47] reaction 4b has also been suggested as the most probable.[29] Solid SiO_2 results after further oxidation and surface reactions of the SiO_xH_y intermediates. This work demonstrates that reactions 1, 2, and 3 are key steps in the overall deposition chemistry. Quantitative mechanistic analysis is presented in our modeling paper.[28]

Results of This Research on SiO_2 Photo-CVD

Absolute r_d's for each oxidant system are presented in Table 1. Very rough estimates of the theoretical r_d's were made using the following nominal reaction stoichiometries:

$$O_2 + h\nu \rightarrow 2O \rightarrow SiO_2 \quad (5)$$

$$H_2O + h\nu \rightarrow OH + H \rightarrow (1/2)SiO_2 \quad (6)$$

$$H_2O_2 + h\nu \rightarrow 2OH \rightarrow SiO_2 \quad (7)$$

with the probability P_{abs} that an oxidant molecule absorbs a photon and photodissociates determined according to

$$P_{abs} = 1 - \exp(-\sigma_{172} n_{ox}) \quad (8)$$

where n_{ox} is the oxidant molecule concentration. The estimated r_d's are about 1.5−2.0 higher than those

(33) Absorption taken from: Okabe, H. *Photochemistry of Small Molecules*; Wiley-Interscience: New York: 1978 and references (H_2O: Watanabe, K.; Zelikoff, M. *J. Opt. Soc. Am.* **1953**, *43*, 753. H_2O_2: Schürges, M.; Welge, K. H. *Z. Naturforsch.* **1968**, *23a*, 1968. O_2: Watanabe, K.; et al. *J. Chem. Phys.* **1953**, *21*, 1026. O_3: Tanaka, Y.; et al. *J. Chem. Phys.* **1953**, *21*, 1651. N_2O: Zelikoff, M.; et al. *J. Chem. Phys.* **1953**, *21*, 1643).

(34) Watanabe, K.; et al. *J. Chem. Phys.* **1953**, *21*, 1026.

(35) Okabe, H. *Photochemistry of Small Molecules*; Wiley-Interscience: New York, 1978.

(36) Anderson, R. W. Private communication.

(37) Yoshino, K.; et al. *Chem. Phys.* **1996**, *211*, 387.

(38) Sawyer, D. T. *Oxygen Chemistry*; Oxford University Press: New York, 1991.

(39) Schürges, M.; et al. *Z. Naturforsch.* **1968**, *23a*, 1968.

(40) Volman, D. H. *J. Chem. Phys.* **1949**, *17*, 947.

(41) Volman, D. H. *J. Photochem. Photobiol. A* **1990**, *51*, 1.

(42) Volman, D. H. *J. Chem. Phys.* **1948**, *16*, 255.

(43) Volman, D. H. *J. Phys. Chem.* **1956**, *25*, 288.

(44) Agrawalla, B. S.; Setser, D. W. *J. Chem. Phys.* **1987**, *86*, 5421.

(45) Atkinson, R.; Pitts, J. N., Jr. *Int. J. Chem. Kinet.* **1987**, *10*, 1151.

(46) Horie, O.; et al. *J. Phys. Chem.* **1991**, *95*, 4349.

(47) Koshi, M.; et al. *J. Phys. Chem.* **1993**, *97*, 4473.

(48) Boyd, I. W. *Mater. Sci. Forum* **1995**, *173−4*, 81.

(49) Ashokan, R.; et al. *J. Appl. Phys.* **1993**, *73*, 3943.

(50) Chapple-Sokol, J. D. In: *SiO_2 and Its Interfaces: Symposium*; Pantelides, S. T., Lucovsky, G., Eds.; Materials Research Society: Pittsburgh, PA, 1988; p 127.

(51) Pai, P. G.; et al. *J. Vac. Sci. Technol., A* **1986**, *4*, 689.

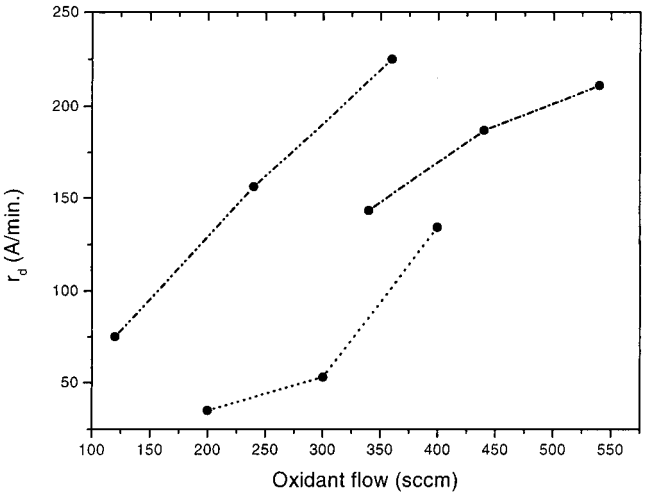

Figure 1. Deposition rates as a function of oxidant flow at 7 Torr (··· ● ···, O_2; −·− ● −·−, H_2O/O_2; −··− ● −··−, H_2O_2). The H_2O/O_2 data are for 240 sccm H_2O plus 100, 200, or 300 sccm O_2.

obtained experimentally. Although the predicted rates compare reasonably well when loss mechanisms such as reaction, diffusion, and dilution are considered, we show in our companion paper that this agreement of the "theoretical deposition rate" and our experiments is largely coincidental.[28]

Examination of Table 1 shows that absolute r_d's with H_2O/O_2 and H_2O_2 are significantly faster than those using only O_2, and higher concentrations of reactants increase r_d's. For example, doubling SiH_4 flow rate raises deposition by 30−35% in the O_2 and H_2O/O_2 systems and 15−25% for H_2O_2. Lower pressures decrease r_d's, and faster flow rates at 5 Torr reduce r_d's and shift the position of the greatest film thickness 3−6 mm downstream, as would be expected with fewer gas phase reactive species impinging on the wafer surface while also having less time to undergo homogeneous reactions. Changes in r_d's as functions of pressure and/or reactant concentrations in the O_2 system follow somewhat nonlinear behavior, whereas changes in the H_2O/O_2 and H_2O_2 systems are more linear. Figure 1, which shows the r_d as a function of oxidant flow at 7 Torr, exemplifies the linear versus nonlinear trends in the different oxidant systems.

For each deposition chemistry, one set of reaction conditions was used to check the effect of purge gas type (where applicable) and temperature. Pressure was fixed at 7 Torr; SiH_4 was fixed at 150 sccm (15% in Ar). The oxidant flows in sccm for the respective chemistries were 300 O_2, 240 H_2O/200 O_2, and 360 H_2O_2. We find that r_d's are only slightly affected by type of purge gas, decreasing slightly when Ar is substituted for N_2. In terms of temperature, r_d's are approximately the same at 75−100 °C, indicating that film formation is driven by photoinduced processes. Increasing substrate temperature increases deposition rate. Arrhenius plots of data obtained for 100−200 °C are depicted in Figure 2. Activation energies (E_a) for the O_2, H_2O_2, and H_2O/O_2 chemistries are 8.8 ± 0.5, 7.6 ± 0.4, and 4.9 ± 0.2 kJ/mol, all of which are much smaller than thermally driven processes. While H_2O and O_2 are thermally stable to high temperatures, thermal decomposition of H_2O_2 may become appreciable at somewhat elevated

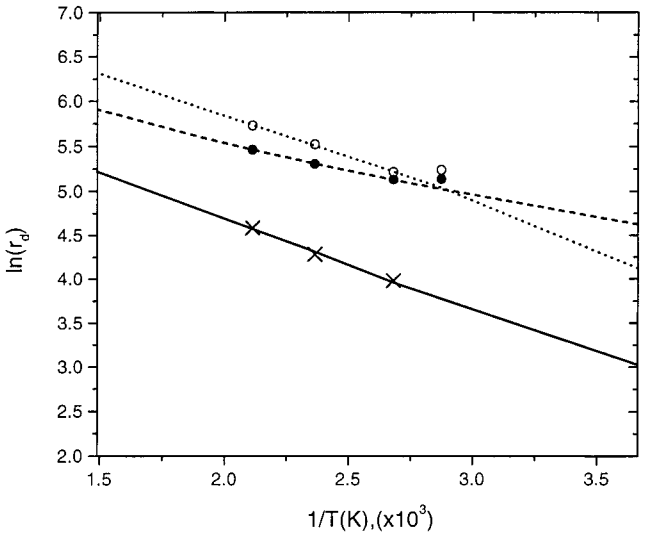

Figure 2. Arrhenius plots for the O_2, H_2O/O_2, and H_2O_2 systems (100−200 °C: −×−, 300 sccm O_2, 9 kJ/mol; ·· ● ··, 240 sccm H_2O + 200 sccm O_2, 5 kJ/mol; − − ○ − − −, 360 sccm H_2O_2, 7.5 kJ/mol).

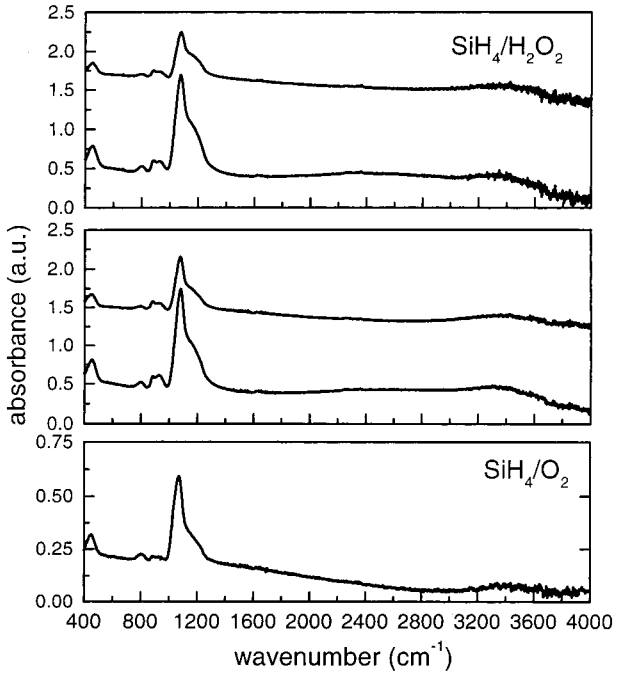

Figure 3. FTIR spectra of SiO_2 films produced by photo-CVD. Upstream (lower line) and downstream (upper line) spectra are shown offset for clarity.

temperatures. However, thermal dissociation of H_2O_2 should cause the deposition profiles to more closely resemble those for H_2O/O_2, and this is not the case (see below).

Representative FTIR spectra are presented in Figure 3, with the position and fwhm of the Si−O absorbance and the nominal film thickness in Table 2. The Si−O stretch consistently lies above 1070 cm^{-1}. All films contain small but detectable amounts of hydrogen,with the lowest amounts in the O_2-based films.

Discussion

The nonlinear trends in deposition as a function of reactant flow and/or pressure and the more conspicuous pressure and oxidant concentration dependence in the

Table 2. Relevant FTIR Data for SiO_2 Films Produced via Each Oxidant Chemistry

system	up- or down-stream	SiO stretch position (cm^{-1})	fwhm (cm^{-1})	nominal film thickness (Å)
SiH_4/O_2	N/A	1072.4	75	5000
$SiH_4/H_2O/O_2$	up	1075	96.4	12 000
	down	1079	90.6	7000
SiH_4/H_2O_2	up	1080	86.8	13 000
	down	1078	75.2	8500

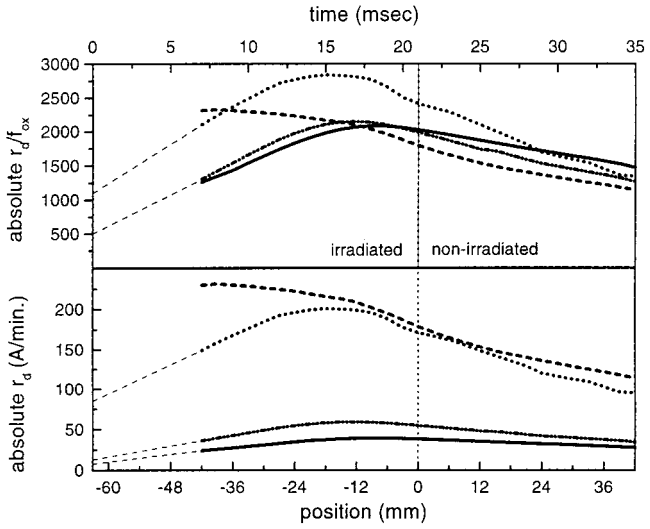

Figure 4. (lower) Deposition profiles of the absolute deposition rates along the wafer surface for the O_2, H_2O/O_2, and H_2O_2 systems (—, 200 sccm O_2; —··—, 300 sccm O_2; ···, 240 sccm H_2O + 200 sccm O_2; - - -, 360 sccm H_2O_2). (upper) Deposition profiles for the O_2, H_2O/O_2, and H_2O_2 systems scaled for differences in VUV absorption (scaling factors: 200 sccm O_2, 0.018; 300 sccm O_2, 0.028; 240 sccm H_2O + 200 sccm O_2, 0.088; 360 sccm H_2O_2, 0.100).

O_2 system suggest that a photoenhanced chain mechanism is operative, with photolysis of one O_2 resulting in more than one SiO_2. The formation of the first Si—O bond by atomic O may produce a partially oxidized Si radical species that is more susceptible to further oxidation by O_2 molecules.[23,36] However, a more important reason is the rapidity of the SiH_3/O_2 reaction (reaction 3). In the H_2O/O_2 and H_2O_2 systems, large concentrations of H_2O may partially mask the effects of varying the relative concentration of the other available photoactive oxidants (either O_2 or H_2O_2).

More information about the reaction chemistry and the nature of the photochemically generated oxidant can be obtained by inspecting the deposition profile along the wafer (i.e., going from the upstream irradiated front edge to the back unirradiated downstream half). This profile may also be considered a time axis. Effects due to processes such as diffusion, incomplete mixing, and/or convection should be approximately the same for all of the reaction systems (conducted at the same pressure and temperature), so profiles should reflect differences in chemistry.

Representative profiles of the r_d's for the three oxidant systems are shown in Figure 4. The lower x-axis shows position along the wafer surface (6-mm increments, up-to downstream); the upper, elapsed time (ms, with t = 0 at $x = -63$ mm). The vertical line at 0 mm indicates the cutoff point of full intensity VUV light. The lower panel plots the absolute r_d's, while in the upper panel, the individual deposition profiles are scaled to provide nominal correction for the fact that each chemical system has different concentrations of oxidant species available from photolysis reactions. The scaling factors are determined by estimating the amount of primary photoproduct relative to undissociated oxidant at any given location along the wafer surface. This is done according to

$$f_{ox} = (Q_{ox}/Q_{flow})nh\sigma_{172} \quad (9)$$

where f_{ox} is the oxidant factor, Q_{ox} and Q_{flow} are the oxidant and total gas flows in sccm, n is the total number density in molecules/cm^3, and h is the maximum height of absorbing gases. The calculated f_{ox} values for O_2 and H_2O_2 are doubled (two O's or two OH's are produced, respectively). Under the reaction conditions indicated, the f_{ox} values are 0.018, 0.028, 0.088, and 0.100 for 200 sccm O_2, 300 sccm O_2, 240 sccm H_2O + 200 sccm O_2, and 360 sccm aqueous H_2O_2, respectively. Both plots show that, in the O_2 system, the peak deposition appears at least 30 mm from the front edge of the wafer. With H_2O/O_2, the peak generally shifts upstream by as much as 6 mm.

Although more details regarding the deposition mechanism are presented in our theoretical paper,[28] some comments are made here regarding the early steps in the process leading to solid-phase SiO_2. When H_2O_2 is used, the deposition peaks near the front edge of the wafer. Both the availability of OH in significant amounts and the chain-type reactions propagated by O_2 appear to be important.

In the O_2 system, O_2 must photodissociate and react with SiH_4 before any OH is produced. As OH concentration builds, so too does the amount of available SiH_3 via reaction 2. SiH_3 is more susceptible to oxidation by O_2 than is SiH_4. A relatively long time must elapse before the latter steps become fully operative, thereby shifting the highest deposition the furthest downstream along the wafer.

With H_2O/O_2, H_2O photolysis provides OH directly, building OH rapidly and thereby generating a greater number of SiH_3 molecules via reaction 2. Reaction 3 then effectively accelerates the deposition process, and peak deposition shifts upstream. The combined effects of rapid SiH_4/OH abstraction reactions and chain-propagation via O_2/SiH_3 probably explain why H_2O/O_2 produces the maximum r_d for a given amount of oxidant/photodissociation.

The highest concentration of OH is available at the earliest times with H_2O_2 via H_2O_2 and H_2O photolysis (two from the former; one from the latter), which can then effect reactions leading to deposition at the front edge of the wafer. The nature of these reactions, however, is unclear. The most likely products of the OH—SiH_4 reaction are SiH_3 and H_2O. Subsequent reactions must generate silicon- and oxygen-containing radical species that can react and/or decompose at the surface to form SiO_2. Such high r_d's so early in the process are unlikely to result from surface reactions between photoproducts of adsorbed oxidants and unoxidized silicon species because deposition should then decrease with increasing temperature. Chain propagation reactions between SiH_3 and H_2O_2 would account for these results,[28] even though the SiH_3–H_2O_2 reaction

does not seem to support the chain mechanism that operates when sufficient O_2 is present. The effects of adding O_2 to the H_2O_2 chemistry are inconclusive because the experiments resulted in powder formation. Another possible explanation lies with the possibility of rapid SiH_4 oxidation by superoxide (HO_2) radical. The relatively fast reaction of OH with H_2O_2 to produce HO_2

$$OH + H_2O_2 \rightarrow HO_2 + H_2O \qquad (10)$$

(1.9×10^{-12} cm^3 molecule^{-1} s^{-1}),[52] could compete with the OH−SiH_4 reaction as long as the H_2O_2 concentration is roughly 10 times that of SiH_4. However, it is unclear what fast chain propagation reaction would utilize HO_2.

In all systems, r_d begins to fall off before the reactants exit the irradiated region. Possible losses include SiH_4 depletion, diffusion (the gases are flowing into a larger volume), and dilution (more purge gas flow is introduced along the wafer surface). The rate of the falloff differs among the three oxidant chemistries, increasing in the order O_2 to H_2O_2 to H_2O/O_2. OH−OH recombination to produce H_2O and O atoms provides a potentially rapid ($k = \sim 2 \times 10^{-12}$)[52] channel for OH loss and could partially account for the falloff in deposition before the gases leave the irradiated region. Evidence to support that this path contributes to the decrease in deposition can be taken from the profiles at 200 and 300 sccm O_2. At the lower O_2 concentration, less OH is produced so the effects of its recombination reactions are less and the decline is slower. OH self-recombination may also partially account for the slow decrease in deposition in the H_2O_2 system over the $x = -42-0$ mm range.

Once the gases leave the irradiated region, photolysis no longer generates active oxidant species. This effect is particularly important in the H_2O-based systems because H_2O photodissociation, an overwhelming contributor to OH production, is shut off. The O_2 system shows the slowest falloff, suggesting that O_2–SiH_3 dark reactions (reaction 2) propagate reactions leading to appreciable deposition. The effects of reaction 2 are probably masked by the large water concentration in the H_2O/O_2 chemistry.

In terms of Ar versus N_2 as purge gas, O(^{1}D) radicals are thought to be among the most effective oxygen radical species reacting with SiH_4, being 1−7 times more reactive than O(^{3}P) or O(^{1}S);[15,53] however, O(^{1}D) undergoes rapid collisional deactivation in the gas phase. Rate constants of O(^{1}D) quenching with Xe, O_2, O_3, CO, CO_2, N_2, NO, N_2O, NO_2, H_2, H_2O, and CH_4 are of the order 10^{-10}−10^{-11} cm^3 molecule^{-1} s^{-1}.[35,52] Ne, Kr, and SF_6 are not good deactivators of O(^{1}D),[54] and He and Ar have been found to be relatively inert.[55,56] Assuming that Ar does not deactivate O(^{1}D) and that N_2 does so efficiently, and depending on the role of O(^{1}D) in the reaction chemistry, significant differences in deposition rates should be evident when Ar is substituted for N_2 if O(^{1}D) is present in significant amounts. The largest effect should occur in the O_2 system.

When O_2 is photolyzed, the mean survival time τ of O(^{1}D) can be estimated by taking the reciprocal of eq 11:

$$k_{O(^1D)} = k_P[P] + k_{O_2}[O_2] \qquad (11)$$

where k_P and k_{O_2} are the deactivation rate constants in purge gas P and oxidant O_2, present in concentrations [P] and [O_2]. The deactivation rate constants for O(^{1}D) in N_2, O_2, and Ar are roughly 2.4×10^{-11}, 2.6×10^{-11}, and 0.1×10^{-11} cm^3 molecule^{-1} s^{-1}, respectively.[52,56] The total concentration of gas species under deposition conditions (about 1.8×10^{17} molecules cm^{-3}) can be used to approximate [P]. For our experiments, τ is about 2.1×10^{-7} s when P = N_2 and about 1.8×10^{-6} s for P = Ar. Hence, O(^{1}D) survives at least 8.5 times longer in Ar, even with an estimate for k_{Ar} that is probably more than an order of magnitude too high. The rate constant for the O(^{1}D)−SiH_4 reaction is not known, but k_{CH_4} for the O(^{1}D)−CH_4 reaction is 1.5×10^{-10} cm^3 molecule^{-1} s^{-1},[52] such that k_{CH_4}/k_{O_2} is close to 6. For these depositions, [O_2]/[SiH_4] is nominally 13. Assuming k_{SiH_4} is roughly the same as k_{CH_4}, O(^{1}D) deactivation by O_2 probably occurs at least twice as often the reaction with SiH_4.

As indicated above, O_2-based r_d's are only slightly affected by purge type, decreasing by about 7% when Ar was substituted for N_2. This suggests that O(^{1}D) is much less important than other oxidant species (e.g., O(^{3}P) or OH) and that, in this case, O(^{1}D)'s higher reactivity does not appear effective in increasing r_d, as hypothesized by other researchers.[15] With H_2O/O_2, the r_d in Ar is about 2% less than in N_2. These findings are also supported by our simulations.[28] Ellipsometric measurements were not taken for films deposited using H_2O_2 in Ar and N_2 for two reasons. First, O(^{1}D) should not be present in appreciable quantities; second, the films obtained in each type of purge gas were essentially indistinguishable.

There are several possible explanations for the small effect of changes in the purge gas. One possibility concerns the branching ratio of O_2 photolysis reactions at 172 nm (production of two O(^{3}P) versus one O(^{3}P) and one O(^{1}D)). The maximum amount of O(^{1}D) available is 50%, but processes such as curve crossing and predissociation might decrease the amount. Another possibility is that a significant fraction of O(^{1}D) reactions with SiH_4 are abstraction reactions rather than insertion reactions.

As mentioned above, VUV photons are required for deposition to occur at 100 °C and below; above 100 °C, r_d's increase with substrate temperature. Over 100−200 °C, activation energies (E_a) extracted from Arrhenius plots for the O_2, H_2O_2, and H_2O/O_2 chemistries are 8.8 ± 0.5, 7.6 ± 0.4, and 4.9 ± 0.2 kJ/mol. The r_d's increase linearly with temperature for H_2O/O_2 and H_2O_2; the O_2 increase is slightly nonlinear. This suggests that the former two proceed essentially without barrier, while the latter might involve a small but nonnegligible activation energy. The E_a associated with the SiH_4/O_2 chemistry observed is fairly close to that obtained by Bergonzo and Boyd (i.e., 12.5 kJ/mol).[16,57] The SiH_4/H_2O/

(52) Atkinson, R.; et al. *J. Chem. Ref. Data* **1997**, *26*, 521. Atkinson, R.; et al. *J. Chem. Ref. Data* **1992**, *21*, 1125.
(53) Chao, S. C.; et al. *J. Electrochem Soc.* **1989**, *136*, 2751.
(54) Horvath, M.; Bilitzky, L.; Hüttner, J. *Ozone*; Elsevier: New York, 1985.
(55) Young, R. A.; et al. *J. Chem. Phys.* **1968**, *49*, 4758.
(56) Yamazaki, H.; et al. *J. Chem. Phys.* **1963**, *39*, 1902.
(57) Taft, E. A. *J. Electrochem. Soc.* **1979**, *126*, 1728.

O_2 and SiH_4/H_2O_2 photoinduced processes have not been investigated by other researchers, so no comparisons can be made. The O_2 shows a residual E_a that is somewhat higher than the H_2O/O_2 and H_2O_2 systems, which is consistent with $k_1 < k_2$. OH may experience a lower barrier to reaction with SiH_4 than $O(^3P)$.

Although we were not able to perform electrical measurements on the films deposited in this work, such measurements will be necessary to confirm the overall suitability of these films for device applications. However, some indication can be drawn from the FTIR results. FTIR spectroscopy represents one of the most valuable ways to quickly and nondestructively inspect film composition and quality qualitatively and/or semiquantitatively.[1] Primary emphasis is placed on the position and fwhm of the absorption associated with the Si−O stretch at around 1070−1080 cm^{-1} because these provide valuable indicators of film stoichiometry and structure. Spectra for stoichiometric films show relatively narrow peaks at wavenumbers in excess of 1070 cm^{-1} for the Si−O stretch. Position usually increases and fwhm decreases as film quality improves. The level of H-containing impurities can be monitored by peaks appearing around 880 and 2000−2300 cm^{-1} for Si−H moieties, and at roughly 920 and 3200−3600 cm^{-1} for OH-type groups.[58−60] With regard to quality, our films show good optical properties when examined visually (i.e., films are clear and not cloudy). The FTIR spectra presented in Figure 3, as well as the data in Table 2, indicate that the Si−O stretch consistently lies above 1070 cm^{-1}. All films show evidence of hydrogen bound as either Si−H or silanol.

The Si−O stretch for a film deposited using 300 sccm O_2, which appears at 1072 cm^{-1} with a fwhm of about 75 cm^{-1}, compares favorably with the value expected for a good, stoichiometric oxide. A low level of OH groups is indicated by the small absorptions at 3200−3600 cm^{-1} and at 920 cm^{-1}. Because no Si−H peaks are evident at 2000−2300 cm^{-1}, the Si−H level is probably near 1 at. % or less.[16,61]

FTIR spectra for representative H_2O/O_2- and H_2O_2-based films (240 H_2O/200 O_2 and 360 H_2O_2) were taken at two locations on the wafer: one upstream (lower line) in the irradiated portion of the sample and one downstream (upper line) in an area not exposed to significant levels of VUV light. In H_2O/O_2 films, the Si−O peak position consistently appears above 1075 cm^{-1}, with fwhm values varying between 91 and 110 cm^{-1}. In the H_2O_2 films, the absorption again appears above 1075 cm^{-1} for all samples, but the fwhm values are narrower than those for the H_2O/O_2 chemistry, being between 75 and 87 cm^{-1}. Changes in the upstream versus downstream spectra for the Si−O−Si stretch are quite small, making it difficult to attribute differences to any one parameter. OH levels are almost impossible to assess because of sloping baselines in the spectra, the noise in the 3200−3600 cm^{-1} region (where Si−OH and H−OH show absorption), and the overlapping absorptions around the 920 cm^{-1} silanol peak. For both oxidant mixtures, the amount of OH in the film appears to slightly increase as the oxidant:SiH_4 ratio increases. Judging from results presented in the literature for SiO_2 films prepared by other methods,[59,60,62,63] OH levels are probably at most 5−10 at. % in all cases.[62] The quality is generally better than SiO_2 films prepared by PECVD.[63] It is difficult to believe that OH content is overwhelmingly high, based on the position and fwhm of the Si−O−Si stretch.

Some speculation can be made regarding the differences in chemistry between the oxidant mixtures. H_2O- and H_2O_2-based films tend to have higher H content than the O_2-based, which makes sense because H atoms are present in these precursors and more OH is available (vs O_2). Surface reactions also provide another possible channel for OH incorporation. H_2O is known to react with strained Si−O−Si bonds and dangling bonds to form silanol groups;[59,60,64] the higher reactivity of H_2O_2 may allow it to act even more effectively in this role.

As a side note, to address the need for low k dielectrics, photo-CVD of low k CH_3-doped SiO_2 from a variety of reactants is being investigated. Initial results appear promising, and further studies are in progress. Work involving VUV-induced curing of spin-on glasses and organosilicates has also proven successful. Results obtained for one type of low k dielectric, methylsilsesquioxane (MSSQ), will be discussed in a separate publication.

Conclusions

This work demonstrates the feasibility of photo-CVD of SiO_2 at low temperatures using a Xe_2* excimer lamp. FTIR analysis and refractive index data suggest that we produced higher quality films using SiH_4/O_2 mixtures than those reported for other Xe_2* excimer lamp based research, and two new oxidant systems enabling high r_d SiO_2 photo-CVD are identified: H_2O/O_2 and H_2O_2. Obtaining films at 100 °C that show Si−O−Si stretch absorptions at 1070 cm^{-1} and higher with no posttreatments (such as annealing at elevated temperatures), at r_d's in excess of 150 Å/min, is remarkable. Mechanistically, the importance of three initial gas-phase reactions is established: $SiH_4 + OH \rightarrow SiH_3 + H_2O$, $SiH_3 + O_2 \rightarrow SiH_3O_2$*, and $SiH_4 + O \rightarrow SiH_3 + OH$. Other notable results include the following: the new H_2O/O_2- and H_2O_2-based chemistries produce higher r_d's than O_2; OH appears to be a prerequisite for significant deposition; a chainlike mechanism based on the SiH_3/O_2 reaction seems to open up when O_2 is present; activation energies are lower when oxidant precursors provide OH directly.

Acknowledgment. We thank Amtech Systems Inc. for significant support of this work. All work was performed in the Department of Chemistry and Biochemistry at the University of California, Santa Cruz, whom we would also like to thank for providing some support for parts of this research. We also acknowledge discussions with Dr. Michael Rhieu about parts of this work.

CM0007095

(58) Boyd, I. W.; Wilson, J. I. B. *J. Appl. Phys.* **1982**, *53*, 4166.
(59) Theil, J. A.; et al. *J. Vac. Sci. Technol., A* **1990**, *8*, 1374.
(60) Theil, J. A.; et al. *J. Electron. Mater.* **1990**, *19*, 209.
(61) Sasella, A.; et al. *J. Vac. Sci. Technol., A* **1997**, *15*, 377.
(62) Pliskin, W. A. *J. Vac. Sci. Technol.* **1977**, *14*, 1064.
(63) Lanford, W. A.; Rand, M. J. *J. Appl. Phys.* **1978**, *49*, 2473.
(64) Parada, E. G.; et al. *J. Vac. Sci. Technol., A* **1996**, *14*, 436.